Data quality of Sentinel-1A IW SLC images and artificial twin backscatterers designed for 3D surface change monitoring with the fusion of PSI and GNSS technologies

László Bányai, Eszter Szűcs and Viktor Wesztergom
MTA Research Centre for Astronomy and Earth Sciences, Sopron, Hungary

Introduction and motivation

The proposal "Integrated Sentinel-1 PSI and GNSS technical facilities and procedures for determination of 3D surface deformations caused by environmental processes" was accepted for implementation by the ESA. The main objective of the proposal is to combine Sentinel-1 IW images processed by integrated Persistent Scatter Interferometry (Ferretti at al. 2001, Hooper et al. 2012) with additional GNSS observations on those important areas, where the use of traditional PSI methods are limited due to complex and unstable ground coverage. This problem can be handled by properly designed artificial backscatterers. If these backscatterers can be used for both ascending and descending satellite passes the vertical and east components of the displacement can be estimated (Savio et al. 2005). These estimates may be biased by the unknown north component. This limitation can be solved by integrated campaign measurements carried out by systematic GNSS observations.

Data and methods

In this paper the primary practical results of the proposal are summarized which are based on the first prototypes of trimmed twin corner reflectors (TCR), which are placed at the Széchenyi István Geophysical Observatory (Fig 1.); and on the result of the processing accomplished with SNAP Sentinel-1 Toolbox provided by the ESA. The TCR is placed on one square meter surface of reinforced concrete block supported by adapters for GNSS, traditional geodetic and gravimetric measurements called as integrated geodetic/geodynamic benchmark. For the test computations the predicted satellite orbits (included in SLC annotation files) and the GNSS derived coordinates of TCR are used, which are given in WGS-84 coordinate system.

Primary results

The identification of TCRs - oriented to the chosen ascending and descending directions - is carried out using the split, deburst and update geo reference modules of the SNAP Sentinel-1 Toolbox. The pixels of TCR can be identified very easily on the VV polarised intensity images. The reflectivities of TCR are 59.9 ±0.6 dB and 29.9 ±5.4 dB for VV and VH polarizations in the ascending cases, respectively, while in the case of descending images they are 60.2 ±0.6 dB and 30.0 ±11.7 dB (Table I). The VH polarizations are worse; sometimes the complex numbers cannot be estimated. The characteristics of the identification of TCRs on the differential interferograms (using coregistration, interferogram formation, deburst, topographic phase removal and update geo reference modules of SNAP) are similar.

The geometric stability of SLC images are investigated by the closest approach method using the predicted orbits and the GNSS measured coordinates of TCR (Table II). The repeatability of ascending images are azimuths ±2 arcsec, incidence angles ±10 arcsec and the differences between the radar derived and measured ranges -5.7 ±1.3 meter. In the case of descending images: azimuths ±2 arcsec, incidence angles ±8 arcsec and range difference -4.7 ±0.6 meter.

Conclusions

These primary results prove that the prototype of the integrated benchmark and the stability of the Sentinel-1A images can fulfil the requirements for the proposed PSI and GNSS data integration. At the moment the missing images, experienced during the test computations, seems to be major limitation, which hopefully will be mitigated when the system will be declared fully operational.
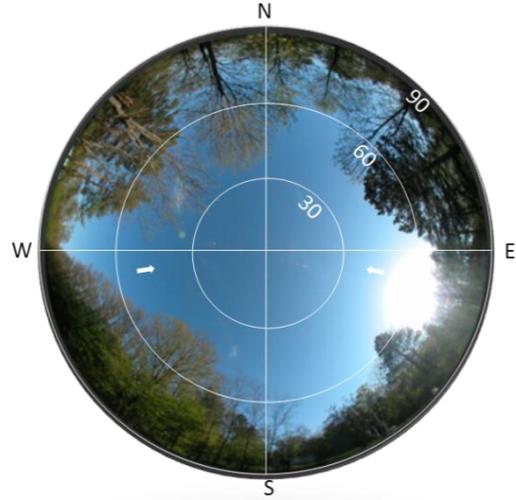
Fig 1. Prototype of trimmed twin corner reflectors (TCR) in the Széchenyi István Geophysical Observatory (left). The white arrows show the azimut and incidence angles of the chosen ascending and descending illuminations on the zenith picture (right).

Table I. The VV and VH polarised intensities of TCR in dB, i and q are the complex numbers

Ascending						Descending					
2015	i	q	VV	i	q	VH	2015	i	q	VV	i	q	VH
6 July	1007	244	60.3	27	NaN	NaN	5 July	-882	542	60.3	23	19	29.5
18 July	-908	517	60.4	57	-37	36.6	17 July	-826	624	60.3	NaN	1	NaN
30 July	64	-909	59.2	-51	-31	35.5	29 July	-911	-256	59.5	77	3	37.7
11 Aug.	-770	712	60.4	-10	17	25.9	10 Aug.		missing image				
23 Aug.	356	1010	60.6	-41	-30	34.1	22 Aug.	-1047	108	60.4	3	-1	10.0
4 Sept.	-680	554	58.9	4	10	20.6	3 Sept.	-766	-851	61.2	56	-8	35.1
16 Sept.	90	-975	59.8	13	-26	29.3	16 Sept.	-94	-946	59.6	51	-56	37.6
28 Sept.	720	-695	60.0	-28	-11	29.6	27 Sept.		missing image				
10 Oct.	-896	-293	59.5	15	19	27.7	9 Oct.		missing image				
mean			59.9			29.9				60.2			30.0
std.			0.6			5.4				0.6			11.7

Table II. The azimuths (α), incidence angels (θ) and differences (Δd) of radar derived and measured SAT-TCR distances.

Ascending				Descending			
2015	α	θ	Δd (m)	2015	α	θ	Δd (m)
6 July	81°08'03"	45°22'03"	-6.1	5 July	279°46'30"	40°20'07"	-5.1
18 July	81°08'05"	45°21'57"	-6.3	17 July	279°46'25"	40°20'00"	-5.6
30 July	81°08'06"	45°21'52"	-2.7	29 July	279°46'29"	40°20'05"	-4.8
11 Aug.	81°08'05"	45°22'04"	-5.8	10 Aug.		missing image	
23 Aug.	81°08'06"	45°22'19"	-6.2	22 Aug.	279°46'31"	40°20'07"	-4.6
4 Sept.	81°08'04"	45°22'19"	-7.5	3 Sept.	279°46'29"	40°20'22"	-4.2
16 Sept.	81°08'04"	45°21'58"	-6.2	16 Sept.	279°46'27"	40°20'14"	-3.9
28 Sept.	81°08'03"	45°21'50"	-5.6	27 Sept.		missing image	
10 Oct.	81°08'06"	45°21'56"	-4.9	9 Oct.		missing image	
mean	81°08'05"	45°22'02"	-5.7		279°46'28"	40°20'09"	-4.7
std.	2"	10"	1.3		2"	8"	0.6

Acknowledgement

References

A Ferretti, C Prati, F Rocca (2001): Permanent scatterers in SAR Interferometry. IEEE TGRS 39 (1)

A Hooper, D Bekaert, K Spaans, M Arikan (2012): Recent advances in sar interferometry time series analysis for measuring crustal deformation, Tectonophysics, 514-517, 1-13.

G Savio, A Ferretti, F Novall, S Musazzi, C Prati, F Rocca (2005): PSInSAR validation by means of a blind experiment using dihedral reflectors. Proc. Fringe 2005 Workshop, Frascatti, Italy